CHEMISTRY
A EUROPEAN JOURNAL

DOI: 10.1002/chem.200902139

Solvent-Induced Structural Transition of Self-Assembled Dipeptide: From Organogels to Microcrystals

Pengli Zhu,[a] Xuehai Yan,[a, b] Ying Su,[a] Yang Yang,[a, c] and Junbai Li*[a]

Abstract: Organogels that are self-assembled from simple peptide molecules are an interesting class of nano- and mesoscale soft matter with simplicity and functionality. Investigating the precise roles of the organic solvents and their effects on stabilization of the formed organogel is an important topic for the development of low-molecular-weight gelators. We report the structural transition of an organogel self-assembled from a single dipeptide building block, diphenylalanine (L-Phe-L-Phe, FF), in toluene into a flower-like microcrystal merely by introducing ethanol as a co-solvent; this provides deeper insights into the phase transition between mesostable gels and thermodynamically stable microcrystals. Multiple characterization techniques were used to reveal the transitions. The results indicate that there are different molecular-packing modes formed in the gels and in the microcrystals. Further studies show that the co-solvent, ethanol, which has a higher polarity than toluene, might be involved in the formation of hydrogen bonds during molecular self-assembly of the dipeptide in mixed solvents, thus leading to the transition of organogels into microcrystals. The structural transformation modulated by the co-solvent might have a potential implication in controllable molecular self-assembly.

Keywords: hierarchical nanostructures · microcrystals · organogels · peptides · self-assembly

Introduction

Successful synthesis of organized supramolecular assemblies is an exciting bottom-up method for fabricating nanostructured materials with novel functional properties.[1–4] The controlled self-assembly of higher-ordered architectures such as those in biological systems, preferably from relatively simple building blocks, is an interesting topic of supramolecular and biomimetic chemistry.[5–13] Peptides, as versatile building blocks that can self-assemble to form well-defined structures, have attracted considerable attention owing to their biocompatibility, capability of molecular recognition, and functional flexibility.[14–24] Among them, the simplest building blocks are aromatic dipeptides, for instance, diphenylalanine (L-Phe-L-Phe, FF), which can self-assemble into discrete and extraordinarily stiff nanotubes in aqueous solutions and then serve as a casting mold for producing metal nanowires.[25,26] Further, FF can be used for the creation of more complex structures, such as vertically aligned nanoforests[27] or nanowires,[28,29] well-organized self-assembled films,[30] and can also be used to order dipeptide chains on Cu surfaces.[31] For instance, the interesting "nanoforest" is a class of ordered nanotube arrays readily fabricated on a siliconized glass by an approach of evaporation-induced self-assembly. The well-ordered organization of nanotubes is most likely controlled by a nucleation-growth mechanism in the vapor–liquid–solid system that exists during the rapid evaporation of solvent.[27]

More recently, our group reported that FF can self-assemble into long nanofibrils in organic solvents such as chloroform, toluene, and xylene, and entangle further to form or-

[a] P. Zhu, Dr. X. Yan, Y. Su, Dr. Y. Yang, Prof. Dr. J. Li
Beijing National Laboratory for Molecular Sciences (BNLMS)
Key Lab of Colloid and Interface Sciences
Institute of Chemistry, Chinese Academy of Sciences
Beijing, 100190 (China)
Fax: (+86) 10-82612629
E-mail: jbli@iccas.ac.cn

[b] Dr. X. Yan
Max Planck Institute of Colloids and Interfaces
Am Mühlenberg 1, 14476, Potsdam/Golm (Germany)

[c] Dr. Y. Yang
National Center for NanoScience and Technology
Beijing, 100190 (China)

Supporting information for this article is available on the WWW under http://dx.doi.org/10.1002/chem.200902139. It contains photographs, AFM images and TGA curves of the samples, X-ray diffraction pattern of the sample prepared at 25% ethanol/toluene mixture, SEM images of the sample obtained in 25% methanol/toluene mixture and dichloromethane, optical images and movie, in situ FTIR and XRD data of microcrystals in solution.

ganogels, which can be used to encapsulate lipophilic quantum dots for the preparation of 3D organic–inorganic architectures with new optical properties.[32] Subsequently, a similar gel system was used to fabricate the 3D colloids by the combination with lipophilic quantum dots for application as label of living cells.[33] A 9-fluorenylmethoxycarbonyl (Fmoc)-protected diphenylalanine (Fmoc-FF) has been presented as a hydrogelator for the fabrication of a hydrogel for 2D or 3D cell culture.[34,35] It is thus well-known that FF has been an excellent self-assembled building block, and is considered to be one of the smallest peptide gelators. Organogels represent new soft matter materials with promising physical and morphological properties and potential applications in fields such as templated materials, separation media, cosmetics, enzyme-immobilization matrices, and drug delivery.[36–38] To form an organogel system, two questions should be considered regarding the molecular structures of the gelators. One is how to prevent the transformation of a metastable gel into a crystalline state, which also represents the fundamental difference between a stable thermodynamic phase and a purely kinetic transition state.[39–42] If the formed gel is unstable, it can spontaneously evolve into crystalline shapes upon ageing.[43–45] The other problem is to choose suitable solvents for the organogelators, because the formation of an organogel is both the result of the gelator–gelator and solvent–gelator interactions, and a given gelator only has the ability to induce macroscopic gelation in certain solvents.[36,40,46,47] Therefore, understanding the precise role of solvent properties on organogel formation is important in designing gels with controlled microscopic structures and physicochemical properties. Considering this point, and by using ethanol as a co-solvent, we can easily control the self-assembly of peptide structures: from organogel to flower-like microcrystals. This not only provides information toward understanding the effect of solvent properties on organogel formation but also represents a facile way to tailor gelator molecules into hierarchical nanostructures.

Results and Discussion

Observation of morphology transition: To gain a direct insight into the self-assembled microstructures, scanning electron microscopy (SEM) was used to observe the resulting dried samples that were prepared at different ethanol/toluene ratios. As we previously reported,[32] a transparent gel was rapidly obtained when a FF/1,1,1,3,3,3-hexafluoro-2-propanol (HFP) solution (20 μL, 0.4 mol) was diluted with toluene to a final concentration of 16 mmol (Figure S1 a in the Supporting Information). Such gels are stable even after several months. As shown in Figure 1 a, the organogel consists of small fibers tens of micrometers long, and these fibers further assemble into thick fiber bundles and then constitute a highly developed, entangled network. Mixing a small amount of ethanol (10 %) into toluene also gives rise to an organogel but with a little opacity. Figure 1 b indicates that the amount and density of fiber bundles decreases noticeably, rendering a network composed of a large number of individual small fibers with width of 70–110 nm. In the system with an ethanol content of 25 %, a semitransparent unstable gel was observed after 10 min. After about 5 h, the gel became inhomogeneous, and white microcrystals appeared. As time passed, the gel shrank further, liquid was exuded, and more microcrystals precipitated. The process for gel–crystal transition upon ageing is outlined in Figure S1 b–d in the Supporting Information. The SEM images reveal that the final precipitates have a flower-like morphology, and they are several hundreds of micrometers in size and composed of ribbons with a width of about 4–5 μm (Figure 1 c, d). The inset in Figure 1 d shows that the surface of the ribbons is smooth. When the ethanol content was increased to 40 %, the system failed to form gels. Instead, visible aggregates appeared in solution after 30 min (Figures S1 e and S2 and movie in the Supporting Information). The morphology of assemblies formed in the 40 % ethanol/toluene mixture almost does not change in comparison to the final microcrystals that were obtained in 25 % ethanol/toluene mixture (Figure 1 e). Upon further increasing the ethanol content to 70 %, only 10 min are needed to get the

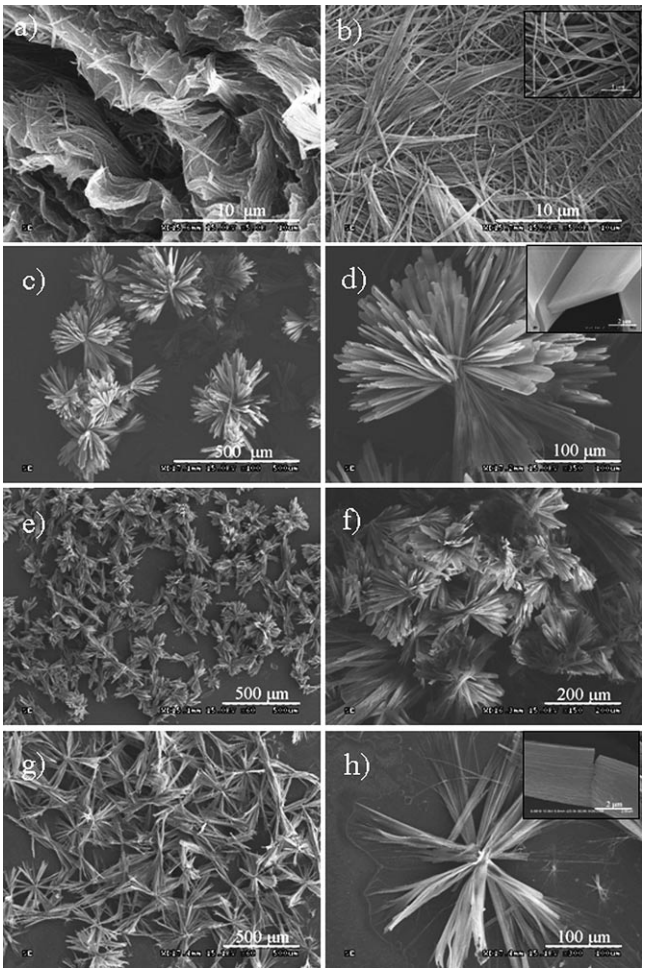

Figure 1. SEM images of samples formed at different ethanol contents: a) 0 %; b) 10 %; c,d) 25 %; e) 40 %; f) 70 %; g,h) 100 %.

flower-like microcrystals (Figure 1f). Figures 1g and 1h show the low- and high-magnification images of the sample prepared by using 100% ethanol as a solvent. It presents many star-like structures with ribbons of 2–4 μm in width. Compared with the above flower-like structures, the density of ribbons in each microcrystal is lower, and the thickness of the ribbons is decreased. The high-magnification image inserted in Figure 1h demonstrates that the surface of the ribbons are rough and loose, so that the electron beam itself provoked the collapse of the ribbons. From the results presented in Figure 1, it is clear that the ratio of ethanol in the mixed solvents has a profound effect on the microscopic structure of the resulting assemblies. When the ethanol content in toluene is changed gradually from 0 to 100%, the corresponding variation (from soft gels to microcrystals) of supramolecular structures self-assembled from FF dipeptide takes place. Also, a spontaneous transition from unstable gels to microcrystals can be achieved by ageing the gels in the 25% ethanol/toluene mixture at room temperature. It should be noted that flower-like microcrystals are directly formed in the bulk phase, mostly by a nucleation-growth process in solution and are not susceptible to a drying process (Figures S2 and S8–S10 in the Supporting Information). That is rather different from the "nanoforest" structures fabricated by Gazit et al., which are grown on the surface of a solid substrate by a fast solvent-evaporation-initiated self-assembly process at high peptide monomer concentration.[27]

To obtain topographical information, the assemblies were further investigated by atomic force microscopy (AFM). The AFM images (Figure 2a and 2b) reveal that the entangled fibers are the main microstructures composing organogels in toluene. As such, the gel system in 10% ethanol/toluene mixture shows predominantly fibrous structures (Figure S3a in the Supporting Information). As shown in Figure 2c and 2d, however, the ribbons become the main microstructures in the crystals when the ethanol content is increased to 40% in mixed solvents. The enlarged AFM image (Figure 2d) indicates that the ribbon in the flower-like microcrystals consists of thin lamellar layers. The AFM images of other microcrystals obtained in 25, 70, and 100% ethanol mixed solvents show the same microstructures (Figure S3b–i in the Supporting Information). From the AFM results, it can be deduced that the microcrystals are formed through the hierarchical self-assembly from the FF molecule merely by changing the co-solvent content.

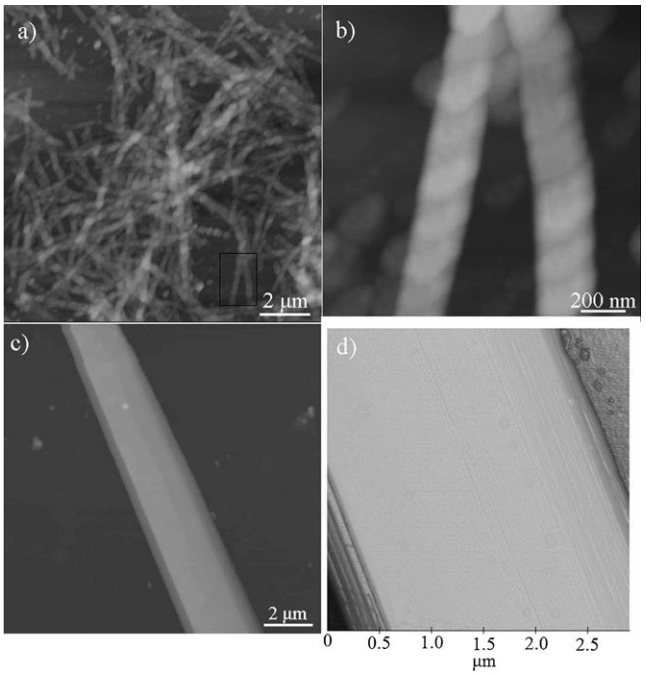

Figure 2. a) Height AFM image of the fibers based on organogel in toluene; b) magnified image of the region marked in image a); c) height AFM image and d) an enlarged 3D-view AFM image of the ribbons of microcrystals obtained in 40% ethanol/toluene mixed solvents.

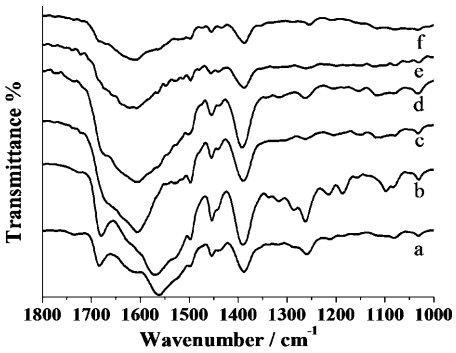

Figure 3. FTIR spectra of different samples: a) dried FF gel in toluene; b) dried FF gel in 10% ethanol/toluene mixed solvents; c–f) microcrystals obtained with ethanol content at 25, 40, 70, and 100%, respectively.

Proposed intermolecular interactions in different structures: Fourier transform infrared spectra (FTIR) were obtained to understand the intermolecular interactions in the dipeptide gel and in the microcrystal state. FTIR spectra of organogels in toluene (Figure 3a) and in 10% ethanol/toluene mixture (Figure 3b) both show a strong amide I absorption band in the vicinity of 1683 cm^{-1}, which is indicative of hydrogen-bonded β-sheet secondary structures, and possibly an antiparallel configuration.[48,49] When the content of ethanol was increased to 25%, the antiparallel β-sheet signals in the gel phase disappeared. Instead, a new peak appeared at 1605 cm^{-1}. This result indicates that the presence of ethanol, to some extent, interferes with the hydrogen bonding from peptide main-chains in the FF gel, thus implying the occurrence of certain structural transitions, which is consistent with the SEM and AFM analysis. Upon further increasing to 70% of ethanol content, the peak shifted to about 1615 cm^{-1}, indicating that the flower-like microcrystals might have a predominant parallel β-sheet configuration.[7,48–50] In the complete ethanol system, the secondary structure of crystals remains unchanged. Therefore, the apparent difference between FTIR spectra of the FF gels and microcrystals suggests that the molecular organization pat-

tern of the dipeptide can be modulated by introducing a solvent with more polarity into the system.

To further understand the diversity of the dipeptide molecular arrangements among the assemblies, fluorescence spectroscopy was used to measure their emission spectra (Figure 4). The emission spectrum of FF at 8 mmol in *N*,*N*-

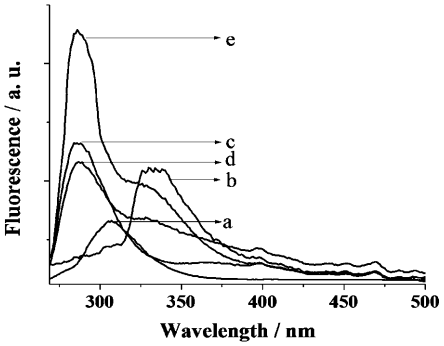

Figure 4. Fluorescence emission ($\lambda_{excitation}$ = 259 nm) of a) a solution of FF in DMF, b) dried gel in toluene, and the microcrystals obtained with ethanol content at c) 25%, d) 70%, and e) 100%, respectively.

dimethylformamide (DMF) shows a signal centered at 306 nm, whereas the emission peak of the dried gel in toluene is near 339 nm. This red shift suggests an effective π–π stacking between the aromatic residues of FF dipeptide molecules, indicating the possible formation of a J-aggregate in the gel.[51–55] In contrast to the gels, the microcrystals obtained with ethanol content of 25, 70, and 100% have the same emission peak at about 285 nm. Compared with the emission spectra of the FF solution and xerogel in toluene, the blue shift possibly indicates a characteristic of an extended H-aggregate between the phenyl rings in the microcrystals.[51–55] In addition, to get a more clear idea about the organization mode of FF aromatic residues, we monitored their absorption spectra in the gel and in absolute ethanol (Figure S4 in the Supporting Information). In comparison with the maximum absorption of free FF molecules (259 nm), a considerable blue shift in ethanol (222 nm) and a red-shifted shoulder around 285 nm in gel further support the conclusions drawn from the emission spectra.[51–55]

X-ray diffraction was used to evaluate the molecular assembly in different samples (Figure 5). Only one sharp peak at 2θ of 5.22 or 5.52°, corresponding to *d* spacing of 16.9 or 15.9 Å, was observed for the xerogel formed in toluene (Figure 5a) and 10% ethanol/toluene mixture (Figure 5b), respectively. The results indicate that the thickness of the β-sheet monolayer in the gel phase is about 1.69 or 1.59 nm. As mentioned previously,[32] the solvent toluene might be involved in the aromatic stacking of FF molecules. Through the addition of a co-solvent with higher polarity (ethanol) in the system, the hydrophobic FF molecules might become more compact and exclude some toluene molecules, so that the *d* spacing of the xerogel in 10% ethanol/toluene mixed solvents is smaller than that in toluene. The XRD pattern

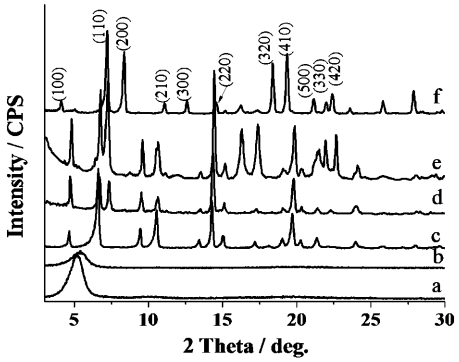

Figure 5. X-ray diffraction of different samples prepared under different ethanol contents: a)–f) represent the samples obtained in ethanol content of 0, 10, 25, 40, 70, and 100%, respectively.

(Figure 5f) of the microcrystals formed in 100% ethanol is very similar to the hexagonal structure determined in a study of FF single crystals and vertically aligned diphenylalanine-based nanotubes (the peak at 28° corresponds to the silicate substrate).[27,30,56,57] The diffraction patterns of the microcrystals formed in 25, 40, and 70% ethanol/toluene mixed solvents (Figure 5c, 5d, and 5e, respectively) are slightly different from the microcrystals obtained from 100% ethanol. Such differences might be contributed to solvent molecules that embedded differently in the crystal lattice depending on the ethanol content, but this proposition needs further substantiation.[43,58]

In the following experiments, we investigated the thermal properties of the microcrystals obtained in different ethanol/toluene mixed solvents. Thermogravimetric analysis (TGA) curves (Figure S5a in the Supporting Information) show that the thermal decomposition of the microcrystals is completed at about 340°C. According to previous reports, the weight loss at 175°C is attributed to release of phenylalanine from diphenylalanine in the assembled nanostructures.[28,29,59] Interestingly, we found that the microcrystals obtained in ethanol content of 25, 40, and 70% have an evident weight-loss step at around 100°C. By comparison, the TGA curve of the microcrystals obtained in 100% ethanol has similar features as that obtained for the FF raw materials, both of which do not have distinctive weight-loss step (Figure 6 and Figure S5b in Supporting Information). Because all of samples were dried until constant weight under vacuum before the TGA measurement, it is rational to suppose that the weight loss at around 100°C corresponds to the release of solvent molecules that are embedded in the crystal lattice of the self-assembly structures of the diphenylalanine. As shown in Figure 6, the weight loss of about 3.5, 3.0, and 2.5% was observed for the microcrystals obtained in 25, 40, and 70% ethanol/toluene mixed solvents, respectively. With the increase of the ethanol content in the mixed solvents, the weight loss of the obtained microcrystals at 100°C is decreased. That is, the higher the toluene ratio in the mixed solvents, the more weight loss is observed at this temperature. This difference is likely due to the interference

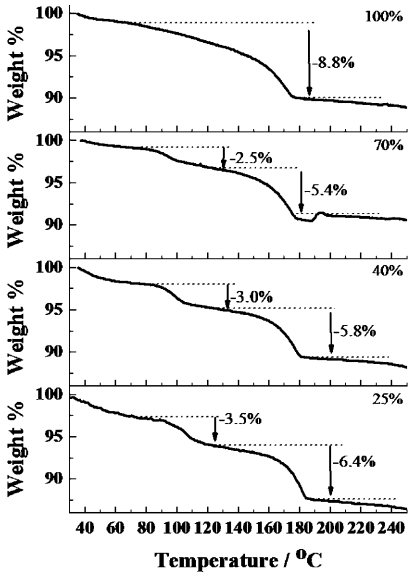

Figure 6. TGA curves between 30–250 °C of the microcrystals obtained in different ethanol/toluene mixed solvents (ethanol content is 100, 70, 40, 25 %, respectively).

of toluene molecules for the self-assembly of diphenylalanine through aromatic stacking. As a consequence, the interaction between solvents and peptide molecules might affect the organization mode of self-assembling dipeptide, which is further confirmed by the slight difference of XRD pattern of the microcrystals (Figure 5c–e). Recent reports showed that an appropriate solvent molecule might be included in the crystal lattice of the simple peptide, and its removal temperature is below the solvent's boiling point.[60–62] In an 100 % ethanol system, the microcrystals have a hexagonal structure. Like the single crystals obtained in the aqueous solution, ethanol molecules might also reside inside the hydrophilic channel formed by hydrophobic FF molecules by hydrogen bonding.[56] Under drying, the ethanol molecules are driven out from the channel so that the weight change upon heating to 100 °C is negligible.

All of the above results indicate that the different molecular organization patterns of the dipeptide can be formed in gels and microcrystals by varying the ratio of ethanol in the mixed solvents. In Scheme 1 the J-aggregate nature of the gel is evident, which is due to the dominant π–π interactions between the aromatic residues of dipeptide molecules in antiparallel β-sheets; the emission of the phenyl groups is red-shifted in contrast to free dipeptide molecules. On the other hand, in the microcrystal, the π–π stacking of the aromatic residues of dipeptide in the parallel β-sheets takes an H-aggregate form and hence leads to the blue-shifted FL emission.

Dynamic morphological transition in the 25 % ethanol/toluene system: From the phenomenon and results of the experiments above, the sample obtained in 25 % ethanol/toluene mixed solvents, which has a gel–crystal transition spontaneously during storage, surprised us very much. As far as we know, there are few examples in which the kinetically trapped state of a gel transfers into a more thermodynamically stable crystal upon ageing. Tang et al.[43] claimed the

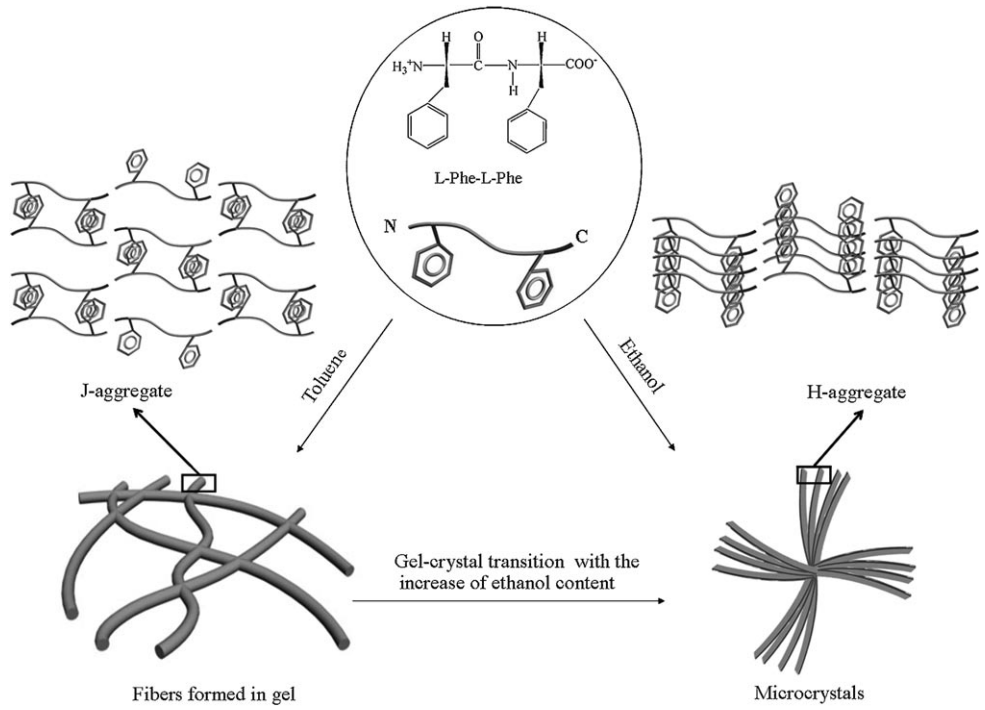

Scheme 1. Schematic illustration of the structural transition induced by varying the ethanol content in the mixed solvents, and the proposed molecular packing in the gel and in the microcrystal.

first example of this transition with a two-component hydrogel. Later, Smith and co-workers[44] reported microcrystallization in a two-component organogel. In this paper, the peptide system is a single component organogel. In addition, the obtained microcrystals have uniform flower-like hierarchical nanostructures. The direct observation by SEM helps us to understand the transition process; for instance, 5 h after the gel formation, some microcrystals were observed in the gel. Figure 7a clearly indicates the existence of

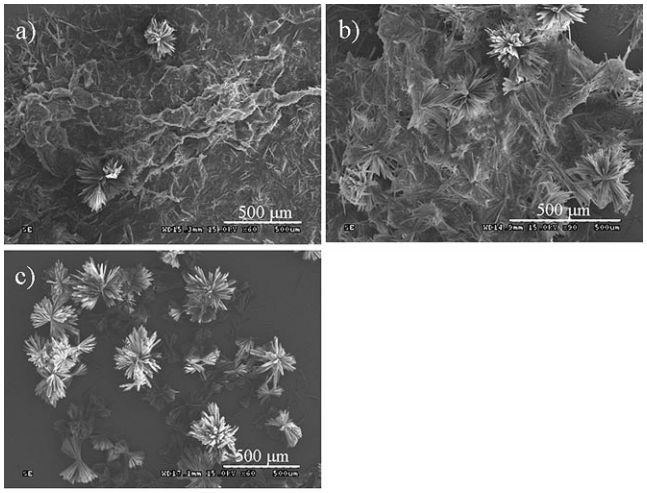

Figure 7. SEM images of the gel–crystal transition process in the 25% ethanol/toluene system as a function of time: a) 5 h; b) 6 h; c) 8 h.

some flower-like microcrystals besides the gel. The XRD pattern at this stage also demonstrates the partial crystallization of the gel (Figure S6 in Supporting Information). After 6 h, more and more microcrystals grew in the system, and some solvent appeared above the gel. This change is induced by the presence of microscale fibers or thin ribbons within the sample (Figure 7b). Furthermore, the gel disappeared completely and microcrystals precipitated (Figure 7c). Previous reports[63] explained that the gel–crystal transformation was related to Ostwald rule of stages. Compared with the crystal, the gel is a metastable state. As strong hydrogen bonds form between ethanol and the dipeptide, isotropic gelator molecular aggregation occurs, resulting in smaller crystals as seen in the gel. The fibers disassemble and dissociate gradually until all the molecules in the gel phase aggregate into larger crystals.

Solvent effects: Owing to the wide-ranging applications of low-molecular-weight organogelators, much effort has been devoted to rational design of gelator molecules.[64] The precise role of the organic solvent in gelating and determining the macroscopic properties of the gel should also be considered because the formation of organogels is both the result of gelator–gelator and solvent–gelator interactions.[36,46] Among the related properties of the solvent, the polarity plays an important role.[46] In general, the organogel can be obtained by using a solvent that has a limited interaction with the gelator molecule.[36] According to the above results, the formation of gel in toluene is driven by the π–π stacking between aromatic residues and hydrogen bonding of peptide main-chains.[32] Compared with toluene, ethanol has a higher polarity and is considered to be a hydrogen-bond donor. The addition of ethanol to toluene increases the polarity of the solvents as well as the solvent–gelator interaction. Therefore, an organogel can only be formed by using a precise proportion of ethanol. As the ratio of ethanol in the mixed solvents is increased, the solvent–gelator interaction, and especially the hydrogen bonding, becomes strong enough to result in the metastable gelator molecular aggregation and the transformation to microcrystals.

To further understand the impact of the polarity of the solvent on the self-assembly of dipeptide, the following experiments were carried out. First, we selected either *n*-butanol or methanol as a component of the co-solvent instead of ethanol, keeping their ratio to toluene in the mixture as 25% (*v*/*v*). *n*-Butanol has lower polarity than ethanol, whereas the polarity of methanol is higher.[65] As we expected, the 25% *n*-butanol/toluene system also has a gel–crystal transition, but the transition takes a much longer time to occur. In the methanol system this transition vanished; only microcrystals appeared gradually. The SEM images show that the morphology of microcrystals is the same as that in 100% ethanol (Figure S7a in Supporting Information). Next, we chose dichloromethane as a substitute, which has higher polarity (comparable with *n*-butanol) than toluene, but has far less ability to provide hydrogen bonding compared with alcohols.[65] When only dichloromethane was used as a solvent for the self-assembly of FF, FF failed to form gels due to the increase of the polarity of solvent. Instead, shuttle-like plates were obtained (Figure S7b in the Supporting Information). But in the 25:75 dichloromethane/toluene mixture and even up to a 90:10 ratio, only stable transparent organogels were formed; this indicates that toluene plays a crucial role for the gelation in the co-solvent. Compared with alcohols, dichloromethane can not take part in the formation of hydrogen bonding between dipeptide molecules because it is neither an acceptor nor a donor for hydrogen bonds, so it does not disrupt the gel formed in the mixed solvents. From above, the polarity of solvent has an influence on the final stable morphology of FF assemblies. Furthermore, the solvent–gelator interaction, especially the hydrogen bonding, is the decisive factor for controlling the gel–crystal transition.

Conclusions

In summary, we have demonstrated that the structural transition from organogels to flower-like microcrystals in the dipeptide self-assembling system can be induced easily by using ethanol as a co-solvent. For the solvent system with 25% ethanol, the spontaneous dynamic transition from organogels into microcrystals has also been confirmed experimentally. In the gel phase the dipeptide molecules are likely

to adopt antiparallel β-sheet secondary structures with the J-aggregate nature of aromatic residues. In the crystalline state, the molecular self-assembled mode is supposed to be the parallel β-sheets and assume the formation of an H-aggregate. The solvent polarity and hydrogen-bonding parameter play important roles in controlling the organogel formation and final self-assembly morphology. The presented results will be advantageous to gain significant new insights into the gelation and self-assembly process of the gelator molecules. Further, such an approach might have potential applications in manipulating the molecular organized pattern and self-assembled morphology by simply changing the solvent properties.

Experimental Section

Materials: The dipeptide (L-Phe-L-Phe, FF), 1,1,1,3,3,3-hexafluoro-2-propanol (HFP), and ethanol were purchased from Sigma–Aldrich (Steinheim, Germany). Toluene was obtained from Beijing Chemical Reagent Corp (Beijing, China) and distilled according to the standard procedures before use. Other solvents were obtained from Beijing chemical Reagent Corp and were used as received.

Formation of organogels and microcrystals: A freshly prepared FF/HFP solution (20 μL, 0.4 mol) was diluted to a final concentration of 16 mmol in toluene or ethanol/toluene mixed solvents. The content of ethanol for different samples was 0, 10, 25, 40, 70, and 100% (*v*/*v*), respectively.

Microscopy studies: The gel or microcrystal samples were carefully picked up and allowed to dry under a vacuum followed by sputtering a thin layer of gold. The images were taken with a S-4300 (HITACHI, Japan) scanning electron microscope. The atomic force microscopy (AFM) images were collected in air at ambient conditions by using the tapping mode with a Nanoscope III a (Digital Instruments, Veeco Metrology Group, Santa Barbara, CA).

Spectroscopy: FTIR spectra were measured by using a TENSOR 27 FTIR spectrometer (Bruker) with the xerogel on a CaF_2 plate, or dried microcrystals were pressed into KBr pellets. A Hitachi Model F-4500 spectrofluorometer was used to measure the fluorescence of the samples. Samples for analysis of gel and microcrystals were prepared on a quartz chip, and a solution of FF in *N*,*N*-dimethylformamide (DMF) was measured in a 1.0 cm quartz cuvette. All the samples were excited at 259 nm.

X-ray diffraction (XRD): Data were collected on a Rigaku D/max-2500 instrument equipped with a Cu filter under the following conditions: scan speed, 2° min^{-1}; $Cu_{K\alpha}$ radiation, $\lambda = 1.5418$ Å. All the samples were prepared on a silica substrate and dried under vacuum.

Thermal analysis: Thermogravimetric analysis (TGA) of the microcrystals was carried out by using a Pyris Diamond TG-DTA (Perkin–Elmer instrument). Samples were heated from RT to 400 °C at a constant rate of 5 K min^{-1} in a N_2 atmosphere. Before the thermal analysis, the as-prepared microcrystals were dried under vacuum until their weights were constant.

Acknowledgements

We acknowledge the financial support of this research by the National Basic Research Program of China (973 program) 2009CB930101 and the National Natural Science Foundation of China (NNSFC20833010) as the German Max-Planck Society collaboration project. X.H.Y. acknowledges support for a research fellowship from the Alexander von Humboldt Foundation. P.L.Z. and X.H.Y. contributed equally to this work.

[1] G. M. Whitesides, J. P. Mathias, C. T. Seto, *Science* **1991**, *254*, 1312–1319.
[2] S. G. Zhang, *Nat. Biotechnol.* **2003**, *21*, 1171–1178.
[3] A. Ajayaghosh, V. K. Praveen, *Acc. Chem. Res.* **2007**, *40*, 644–656.
[4] S. S. Babu, V. K. Praveen, S. Prasanthkumar, A. Ajayaghosh, *Chem. Eur. J.* **2008**, *14*, 9577–9584.
[5] C. Du, G. Falini, S. Fermani, C. Abbott, J. Moradian-Oldak, *Science* **2005**, *307*, 1450–1454.
[6] Z. Y. Tian, Y. Z. Zhang, Y. Ma, W. S. Yang, Y. Chen, Y. L. Tang, J. N. Yao, *Colloids Surf.* **2005**, *269*, 16–21.
[7] N. S. de Groot, T. Parella, F. X. Aviles, *Biophys. J.* **2007**, *92*, 1732–1741.
[8] J. D. Hartgerink, E. Beniash, S. I. Stupp, *Science* **2001**, *294*, 1684–1688.
[9] S. Mann, *Nature* **1993**, *365*, 499–505.
[10] S. Mann, *Angew. Chem.* **2000**, *112*, 3532–3548; *Angew. Chem. Int. Ed.* **2000**, *39*, 3392–3406.
[11] H. Cölfen, S. Mann, *Angew. Chem.* **2003**, *115*, 2452–2468; *Angew. Chem. Int. Ed.* **2003**, *42*, 2350–2365.
[12] H. T. Shi, J. M. Ma, H. M. Cheng, *J. Am. Chem. Soc.* **2003**, *125*, 3450–3451.
[13] Q. Y. Lu, F. Gao, S. Komarneni, *J. Am. Chem. Soc.* **2004**, *126*, 54–55.
[14] X. H. Yan, Q. He, K. W. Wang, L. Duan, Y. Cui, J. B. Li, *Angew. Chem.* **2007**, *119*, 2483–2486; *Angew. Chem. Int. Ed.* **2007**, *46*, 2431–2434.
[15] M. R. Ghadiri, J. R. Granja, L. K. Buehler, *Nature* **1994**, *369*, 301–304.
[16] D. T. Bong, T. D. Clark, J. R. Granja, M. R. Ghadiri, *Angew. Chem.* **2001**, *113*, 1016–1041; *Angew. Chem. Int. Ed.* **2001**, *40*, 988–1011.
[17] J. D. Hartgerink, E. Beniash, S. I. Stupp, *Proc. Natl. Acad. Sci. USA* **2002**, *99*, 5133–5138.
[18] X. Y. Gao, H. Matsui, *Adv. Mater.* **2005**, *17*, 2037–2050.
[19] E. Gazit, *Chem. Soc. Rev.* **2007**, *36*, 1263–1269.
[20] S. Vauthey, S. Santoso, H. Gong, N. Watson, S. G. Zhang, *Proc. Natl. Acad. Sci. USA* **2002**, *99*, 5355–5360.
[21] S. G. Zhang, D. M. Marini, W. Hwang, S. Santoso, *Curr. Opin. Chem. Biol.* **2002**, *6*, 865–871.
[22] Y. J. Song, S. R. Challa, C. J. Medforth, Y. Qiu, R. K. Watt, D. Pena, J. E. Miller, F. van Swol, J. A. Shelnutt, *Chem. Commun.* **2004**, 1044–1045.
[23] S. Santoso, W. Hwang, H. Hartman, S. G. Zhang, *Nano Lett.* **2002**, *2*, 687–691.
[24] X. H. Yan, Y. Cui, Q. He, K. W. Wang, J. B. Li, W. H. Mu, B. L. Wang, Z. C. Ou-yang, *Chem. Eur. J.* **2008**, *14*, 5974–5980.
[25] M. Reches, E. Gazit, *Science* **2003**, *300*, 625–627.
[26] O. Carny, D. E. Shalev, E. Gazit, *Nano. Lett.* **2006**, *6*, 1594–1597.
[27] M. Reches, E. Gazit, *Nat. Nanotechnol.* **2006**, *1*, 195–200.
[28] J. Ryu, C. B. Park, *Adv. Mater.* **2008**, *20*, 3754–3758.
[29] J. Ryu, C. B. Park, *Chem. Mater.* **2008**, *20*, 4284–4290.
[30] N. Hendler, N. Slidelman, M. Reches, E. Gazit, Y. Rosenberg, S. Richter, *Adv. Mater.* **2007**, *19*, 1485–1488.
[31] Y. Wang, M. Lingenfelder, T. Classen, G. Costantini, K. Kern, *J. Am. Chem. Soc.* **2007**, *129*, 15742–15743.
[32] X. H. Yan, Y. Cui, Q. He, K. W. Wang, J. B. Li, *Chem. Mater.* **2008**, *20*, 1522–1526.
[33] X. H. Yan, Y. Cui, W. Qi, Y. Su, Y. Yang, Q. He, J. B. Li, *Small* **2008**, *4*, 1687–1693.
[34] V. Jayawarna, M. Ali, T. A. Jowitt, A. E. Miller, A. Saiani, J. E. Gough, R. V. Ulijn, *Adv. Mater.* **2006**, *18*, 611–614.
[35] A. Mahler, M. Reches, M. Rechter, S. Cohen, E. Gazit, *Adv. Mater.* **2006**, *18*, 1365—1370.
[36] G. Y. Zhu, J. S. Dordick, *Chem. Mater.* **2006**, *18*, 5988–5995.
[37] P. Terech, R. G. Weiss, *Chem. Rev.* **1997**, *97*, 3133–3160.
[38] D. J. Abdallah, R. G. Weiss, *Adv. Mater.* **2000**, *12*, 1237–1247.
[39] P. Terech, N. M. Sangeetha, U. Maitra, *J. Phys. Chem. B* **2006**, *110*, 15224–15233.

[40] K. Hanabusa, M. Matsumoto, M. Kimura, A. Kakehi, H. Shirai, *J. Colloid Interface Sci.* **2000**, *224*, 231–234.
[41] J. D. Rudder, B. Berge, H. Berghmans, *Chem. Phys.* **2002**, *275-285*, 2083–2088.
[42] N. M. Dixit, C. F. Zukoski, *Phys. Rev.* **2003**, *67*, 061501.
[43] Y. J. Wang, L. M. Tang, J. Yu, *Cryst. Growth Des.* **2008**, *8*, 884–889.
[44] J. R. Moffat, D. K. Smith, *Chem. Commun.* **2008**, 2248–2250.
[45] J. Makarevic, M. Jokic, B. Peric, V. Tomisic, B. K. Prodic, M. Zinic, *Chem. Eur. J.* **2001**, *7*, 3328–3341.
[46] A. R. Hirst, D. K. Smith, *Langmuir* **2004**, *20*, 10851–10857.
[47] G. John, J. H. Jung, M. Masuda, T. Shimizu, *Langmuir* **2004**, *20*, 2060–2065.
[48] K. Elfrink, J. Ollesch, J. Söhr, D. Willbold, D. Riesner, K. Gerwert, *Proc. Natl. Acad. Sci. USA* **2008**, *105*, 10815–10819.
[49] M. S. Lamm, K. Rajagopal, J. P. Schneider, D. J. Pochan, *J. Am. Chem. Soc.* **2005**, *127*, 16692–16700.
[50] A. Barth, C. Zscherp, *Q. Rev. Biophys.* **2002**, *35*, 369–430.
[51] S. Gadde, E. K. Batchelor, J. P. Weiss, Y. H. Ling, A. E. J. Kaifer, *J. Am. Chem. Soc.* **2008**, *130*, 17114–17119.
[52] G. F. Lu, Y. L. Chen, Y. X. Zhang, M. Bao, Y. Z. Bian, X. Y. Li, J. Z. Jiang, *J. Am. Chem. Soc.* **2008**, *130*, 11623–11630.
[53] M.-S. Choi, *Tetrahedron Lett.* **2008**, *49*, 7050–7053.
[54] A. M. Smith, R. J. Williams, C. Tang, P. Coppo, R. F. Collins, M. L. Turner, A. Saiani, R. V. Ulijn, *Adv. Mater.* **2008**, *20*, 37–41.
[55] A. Ajayaghosh, C. Vijayakumar, R. Varghese, S. J. George, *Angew. Chem.* **2006**, *118*, 470–474; *Angew. Chem. Int. Ed.* **2006**, *45*, 456–460.
[56] C. H. Görbitz, *Chem. Eur. J.* **2001**, *7*, 5153–5159.
[57] C. H. Görbitz, *Chem. Commun.* **2006**, 2332–2334.
[58] D. K. Kumar, D. A. Jose, A. Das, P. Dastidar, *Chem. Commun.* **2005**, 4059–4061.
[59] V. L. Sedman, L. Adler-Abramovich, S. Allen, E. Gazit, S. J. B. Tendler, *J. Am. Chem. Soc.* **2006**, *128*, 6903–6908.
[60] M. Akazome, T. Takahashi, R. Sonobe, K. Ogura, *Tetrahedron* **2002**, *58*, 8857–8861.
[61] M. Akazome, Y. Ueno, H. Ooiso, K. Ogura, *J. Org. Chem.* **2000**, *65*, 68–76.
[62] M. Akazome, K. Senda, K. Ogura, *J. Org. Chem.* **2002**, *67*, 8885–8889.
[63] V. J. Anderson, H. N. W. Lekkerkerker, *Nature* **2002**, *416*, 811–815.
[64] S. Debnath, A. Shome, S. Dutta, P. K. Das, *Chem. Eur. J.* **2008**, *14*, 6870–6881.
[65] L. Malavolta, E. Oliverira, E. M. Cilli, C. R. Nakaie, *Tetrahedron* **2002**, *58*, 4383–4394.

Received: July 31, 2009
Published online: January 29, 2010

